THE ASTROPHYSICAL JOURNAL, 516:L61–L64, 1999 May 10

EFFECTIVE RADII AND COLOR GRADIENTS IN RADIO GALAXIES

ASHISH MAHABAL[1] AND AJIT KEMBHAVI
Inter-University Centre for Astronomy and Astrophysics, Post Bag 4, Ganeshkhind, Pune, 411 007, India
AND
P. J. MCCARTHY
Observatories of the Carnegie Institute of Washington, 813 Santa Barbara Street, Pasadena, CA 91101-1292
Received 1998 May 20; accepted 1999 March 5; published 1999 March 19

ABSTRACT

We present de Vaucouleurs's effective radii in *B* and *R* bands for a sample of Molonglo Reference Catalogue radio galaxies and a control sample of normal galaxies. We use the ratio of the scale lengths in the two bands as an indicator in order to show that the radio galaxies tend to have an excess of blue color in their inner region much more frequently than the control galaxies do. We show that the scale length ratio is a useful indicator of radial color variation, even when the conventional color gradient is too noisy to serve the purpose.

Subject headings: galaxies: active — galaxies: structure

1. INTRODUCTION

Traditionally, radio galaxies were believed to be elliptical galaxies that consisted of a coeval population of old stars and almost no dust or gas. However, detailed photometric studies in the optical band, as well as X-ray observations, have demonstrated that elliptical galaxies, especially those hosting radio sources, not only have significant quantities of dust and gas but also possess fine morphological structure indicating some amount of activity in the past $\sim 10^2$ million years (see, e.g., Smith & Heckman 1989). Radio galaxies host an active galactic nucleus (AGN) and also have radio jets that transport a very large amount of energy over hundreds of kiloparsecs. Such phenomena are likely to be associated with morphological features and star formation activity not found in normal elliptical galaxies.

In this Letter, we present the main results from a detailed morphological study of a sample of radio galaxies from the Molonglo Reference Catalogue (MRC). We present de Vaucouleurs's effective radii (scale lengths), obtained from careful model fits to surface brightness profiles of the galaxies, and show that the ratio $r_e(B)/r_e(R)$ of the scale lengths in *B* and *R* filters provides a measure of the color gradient in the galaxy. The ratio is related to color gradients measured conventionally but is more robust: it can provide an estimate of the color gradient even when the signal-to-noise ratio is not good enough for the color gradient to be measured unambiguously using the conventional technique. Using the ratio, we show that a large fraction of radio galaxies become bluer toward the center.

2. SAMPLE AND OBSERVATIONS

Our results are based on the observations of 30 galaxies from the MRC that have 408 MHz radio flux $S_{408} > 0.95$ Jy, redshift $z < 0.3$, and declination $-30° \leq \delta(1950) \leq -20°$. The objects were observed from the Las Campanas Observatory, Chile, in 1995 January and 1996 February using the 1.0 m f/7 Swope telescope and the 2.5 m f/7.5 du Pont telescope. Images were obtained in Johnson's *B* and Cousin's *R* filters, which are centered at 0.44 and 0.65 μm, respectively, and have a bandwidth of $\sim$0.1 μm. The typical exposure time was $\sim$20 minutes in *R* and $\sim$60 minutes in *B*. The FWHM of the point-spread function (PSF) ranged from $\sim 1\farcs1$ to $\sim 1\farcs5$. When the FWHM of the PSF was different for the images in the *B* and *R* filters for the same object, the better PSF was degraded to match the other before it was used to compare properties that involve both the filters. The plate scale was $0\farcs7$ pixel^{-1}, and the total field of view covered in an exposure was $11\farcm5 \times 11\farcm5$ in 1995 January and $23' \times 23'$ in 1996 February. The large field allowed us to determine the sky background more accurately than is usually possible. All the processing was done in the normal way using tasks from IRAF and STSDAS, and the details will be published elsewhere (Mahabal, Kembhavi, & McCarthy 1999).

For the purpose of comparison, we extracted a control sample from the CCD fields of our radio galaxies. The sample consists of all nonradio, early-type galaxies from the fields that have semimajor axis lengths greater than 15″. There are 30 galaxies in the control sample, and these were processed and analyzed in a fashion identical to the radio galaxies. The redshifts for the galaxies in the control sample are not known. However, the distribution of angular sizes and apparent magnitudes for the control sample are similar to that of the radio sample, and hence the redshift distributions for the two samples are unlikely to be too different. Our main results, based on the ratio of scale lengths in the *B* and *R* filters, are unlikely to be affected by any small changes in the redshift distribution.

3. SURFACE PHOTOMETRY

We fitted the isophotes of each galaxy in both the *B* and *R* filters with a succession of ellipses with different semimajor axis lengths by using tasks in IRAF that are based on the algorithm described by Jedrzejewski (1987). The mean surface brightness for the series of best-fit ellipses gives us the radial surface brightness profile of a galaxy as a function of the semimajor axis length. From the radial profile in the two bands, we obtained the $B - R$ color profile for each galaxy.

Major contributions to the galactic light can, in general, come from a spheroidal bulge and a flattened disk. In active galaxies, an additional substantial contribution to the central region can be made by the AGN acting as a point source. The relative strengths of the components vary over galaxy type and can be determined by fitting the observed radial surface brightness

[1] Present address: Physical Research Laboratory, Astronomy and Astrophysics Division, Navrangpura, Ahmedabad, 380 009, India.

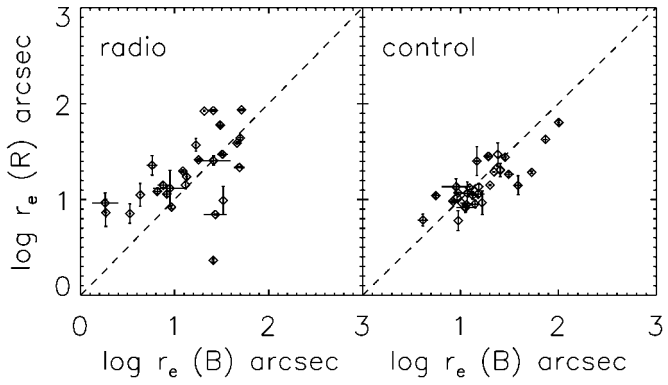

FIG. 1.—The r_e in B and R filters for the radio sample (*left*) and the control sample (*right*). The dashed line is the locus $r_e(B) = r_e(R)$. The points above it denote galaxies that become bluer inward. There is a larger number of such cases among the radio galaxies.

profile of the galaxy with a composite model made up of contributions from each component.

We have assumed that the bulge profile is described by de Vaucouleurs's law, and the disk profile by an exponential. The contribution of the AGN corresponds to a point source broadened by the point-spread function. We have found for our sample of radio galaxies that the AGN is too weak to be detected unambiguously and too weak to be distinguished from other compact features that may be present. We therefore do not include an AGN in our fits. The model surface brightness $I(r)$ at a semimajor axis length r is then given by

$$I(r) = I_e \exp\{-7.67[(r/r_e)^{1/4} - 1]\} + I_d \exp(-r/r_d), \quad (1)$$

where I_e is the bulge intensity at de Vaucouleurs's effective radius (scale length) r_e, I_d is the disk surface brightness at $r = 0$, and r_d is the disk scale length; de Vaucouleurs's law is known to provide a good fit over the range $0.1r_e < r < 1.5r_e$ (Burkert 1993). The points that we use in our fits lie in this range.

To obtain the best-fit model to an observed galaxy profile, we generate a model galaxy with a two-dimensional surface brightness distribution corresponding to trial values of the four parameters in equation (1) and observed bulge and disk ellipticities. We convolve the model with a Gaussian PSF determined from the observed frames for the galaxy in question, and then we obtain the model radial profile. We determine the best-fit parameters by minimizing the reduced χ^2 function $\chi^2_\nu = \sum (I_o - I_m)^2/\nu\sigma^2$, where I_o and I_m are the observed and model surface brightnesses, respectively, at specific distances along the semimajor axis. The standard deviation σ at each point is obtained from the ellipse-fitting task in IRAF and includes photon-counting as well as ellipse-fitting errors; ν is the number of degrees of freedom and is equal to the number of points used in the fit, reduced by the number of free parameters.

Contributions to χ^2_ν are obtained at semimajor axis lengths r in the range $r_1 < r < r_2$, where the inner limit r_1 is chosen such that it lies at a radial separation of 1.5 times the FWHM of the PSF and the outer limit r_2 is chosen such that $\sigma(I)/I$ drops to 0.1. We have omitted the points inside r_1, which typically involve just a few pixels, from the fit because the profile here can be seriously affected by the PSF as well as by any departures from de Vaucouleurs's law that may be present close to the center. The PSF influences the shape of the profile to several times the FWHM (see Franx, Illingworth, & Heckman 1989 and Peletier et al. 1990), but we account for this in our work by convolving the model profile with a model PSF before comparing it with the observed profile. We have carried out runs on artificial galaxies (created using the IRAF package ARTGAL) and on nearby elliptical galaxies and galaxies from our sample suggesting that the value of the extracted effective radius stabilizes beyond 1.5 times the PSF FWHM (Mahabal 1998), when PSF-convolved profiles are used.

We have fitted the bulge plus disk combination in equation (1) to the radio galaxies. In many cases, the ratio D/B of the disk-to-bulge luminosity is $\ll 1$, which is consistent with the radio galaxies being elliptical. In some cases, we detect a disk component $D/B \geq 0.3$, but the disk scale length is small, except in two cases, so that the detected "disk" is a small-scale structure unlike the disks in spiral galaxies. We will describe elsewhere our findings regarding the disklike structures; we devote our attention here to the bulges. Pure bulge fits also turn out to be acceptable in most cases, but the disk plus bulge fits provide better χ^2_ν values on the whole, and we retain them since one of our aims in the larger investigation has been to find any disklike structures that may be present. The results reported here would not change if pure bulge fits were used in the discussion. None of the control galaxies have a significant disk component.

3.1. *Goodness of Fit*

We get very good ($\chi^2_\nu < 1$) or acceptable ($1 < \chi^2_\nu < 2$) fits in ~85% of the cases for the radio as well as the control sample. Visually too, less than ~10% of the galaxies are seen to be highly distorted in the radio sample. It follows that strong radio sources *do not* prefer highly distorted galaxies; χ^2_ν does not increase as a function of redshift; i.e., we get good fits right up to the redshift of 0.3 that we have considered. We find that $\chi^2_\nu(B)$ values are, in general, smaller than the corresponding $\chi^2_\nu(R)$ values. The lower values in B are partly due to the higher σ-values there. It also appears that isophote-distorting influences like the emission and absorption regions, which could increase $\chi^2_\nu(B)$, are averaged out in the ellipse and profile fits.

3.2. *Bulge Parameters*

We now turn to the bulge scale lengths. Figure 1 shows a plot of $r_e(B)$ against $r_e(R)$ for the radio and control galaxies. The 1 σ errors on r_e, obtained from the fitting program, are typically ~10%. The scale lengths in the two filters are equal to within 1 σ in several cases, and these values are scattered around the $r_e(B) = r_e(R)$ line in the figure. In the other cases, we have $r_e(B) < r_e(R)$ (points above the equality line) or $r_e(B) > r_e(R)$ (points below). It is obvious from the figure that the former are more numerous in the radio galaxies, while the latter occur more frequently in the control galaxies.

When $r_e(B) > r_e(R)$, the surface brightness in R increases more rapidly toward the center than the surface brightness in B. In other words, from the definition of the effective radius r_e, half the red light from the galaxy is contained in a smaller region than half the blue light. Therefore, $r_e(B) > r_e(R)$ implies that, on the average, the galaxy becomes redder inward. Similarly, when $r_e(B) < r_e(R)$, the galaxy becomes bluer as one moves toward the center. The distribution of points in Figure 1 therefore shows that the radio galaxies become bluer toward the center more often than the control galaxies.

We have shown in Figure 2 the distribution of the ratio $r_e(B)/r_e(R)$ for the radio and control galaxies. An application

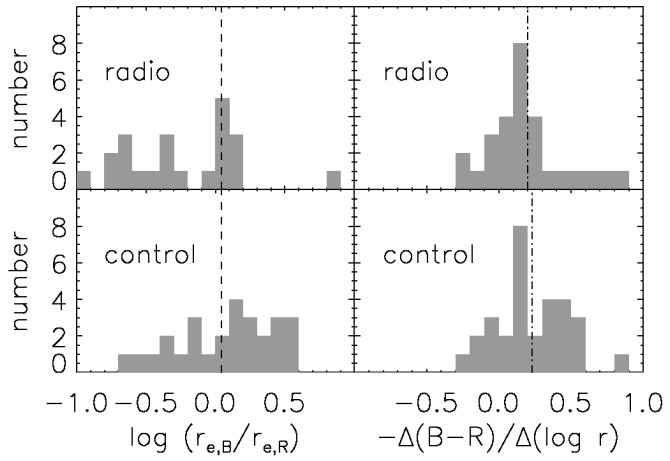

FIG. 2.—The distribution of $r_e(B)/r_e(R)$ (*left*) and the color gradient (*right*) for the radio and control samples. The negative numbers on the *x*-axis are indicative of galaxies with excess blue emission toward the center.

of the Kolmogorov-Smirnov test shows that the two distributions are different at the 99.99% confidence level. For the radio sample, the mean value of the ratio is $\langle r_e(B)/r_e(R)\rangle_r = 0.87 \pm 0.15$, while for the control sample, the mean value is $\langle r_e(B)/r_e(R)\rangle_c = 1.25 \pm 0.10$. The larger value of the ratio for the control sample is consistent with previous studies of early-type galaxies, which show that their colors become redder inward (see, e.g., Sandage & Vishwanathan 1978). Contrary to this behavior, the distribution of the bulge scale length ratio for the radio galaxies shows that they tend to become bluer as one moves toward their inner region; i.e., the color variation in radio galaxies is opposite of that in the control galaxies. In the next section, we will consider the relation between the scale length ratio and the conventional color gradient.

From the profile fits, we have excluded points within 1.5 times the FWHM of the PSF from the center. For our sample, the excluded region has a physical dimension extending to ~4 kpc at the highest redshift. It follows that the inner bluer color of the radio galaxies is not due to a blue AGN or any other unresolved features at the center but must arise in regions that are spread out.

4. COLOR GRADIENTS

The color variation in a galaxy is normally measured by a color gradient parameter $G \equiv \Delta(B-R)/\Delta(\log r)$. The change in color per decade in radius is almost linear in most galaxies, and G is obtained by fitting a straight line to the color profile between an inner radius r_1 and an outer radius r_2. We choose these radii, as described in § 3, with the additional caveat that now $r_2 = \min[r_2(B), r_2(R)]$.

When two small galaxies (angular diameter less than 15″) and a quasar host in our radio sample are excluded, we find that the mean color gradients, in magnitudes per arcsec^2 per decade in radius, for the radio and control samples are $\langle G\rangle_r = -0.20 \pm 0.05$ and $\langle G\rangle_c = -0.23 \pm 0.05$, respectively. The distribution of gradients is shown in Figure 2. We find that the numbers that we obtain are larger in magnitude than those obtained by other authors. For a sample of normal elliptical galaxies (with dusty galaxies excluded), Peletier et al. (1990) had obtained a color gradient of -0.1. Zirbel (1996) had obtained a value of -0.15 for a sample of radio galaxies.

TABLE 1

COLOR GRADIENT DETAILS FOR THE TWO SAMPLES[a]

	FROM COLOR PROFILE		FROM SCALE LENGTHS	
COLOR GRADIENT	Radio	Control	Radio	Control
Less than 0	20	24	9	20
Greater than 0	7	6	18	10
Uncertain	3	0	3	0

[a] As obtained from the color profile and from the bulge scale lengths. A negative color gradient is indicative of a redder center relative to the outer regions.

However, we have confirmed that the larger numbers we get are not due to photometric errors.

4.1. *Color Gradients and Scale Length Ratios*

Color gradients and scale length ratios are both indicative of the change in color with distance from the center, and they are related, to a first approximation, by

$$G \equiv \frac{\Delta(B-R)}{\log(r_2/r_1)} \simeq \frac{2.06(r_2^{1/4} - r_1^{1/4})}{r_e(B)^{1/4}\log(r_2/r_1)}\left[1 - \frac{r_e(B)}{r_e(R)}\right]. \quad (2)$$

For galaxies that obey de Vaucouleurs's law, the color gradient can therefore be estimated from the fitted bulge scale lengths. We enumerate in Table 1 the distribution of color gradients obtained using the scale lengths as well as the gradients obtained directly from the color profiles using the measured values of the $B-R$ color at r_1 and r_2. We have deviated from the more usual custom of taking the outer point at r_e since, in some cases, the color profile is very noisy at that radius. The gradient does not change very much with changes in r_1 and r_2. It is seen from the table that the color gradients obtained directly from the color profiles have a different distribution from the bulge scale length–related color gradient. The distribution of the latter clearly shows that radio galaxies become bluer toward the center while the control galaxies become redder. This distinction is not obvious from the distribution of the directly measured color gradient. In Figure 3, we have plotted the conventional color gradient against that obtained from the scale lengths for the radio galaxies. A simple 2 × 2 contingency test shows that the two color indicators vary in the same sense.

The conventional color gradient is obtained by fitting a straight line to the color profile, which neglects any curvature that may be present. Also, due to the limited signal-to-noise ratio available, often the errors on the color gradient can be large, making the measured values uncertain. The process of obtaining scale lengths involves averaging over isophotes as well as the profile fit with an empirically tested model. We have seen above that the χ^2_ν obtained are well within acceptable limits in most cases for good fits. The scale lengths are therefore good, robust indicators of the large-scale distribution of light in the galaxy, and their ratio in the two filters provides a useful descriptor of the way the color changes over the galaxy. Using the ratio, we have demonstrated the ubiquity of inner blue color in radio galaxies, a fact that is not apparent from the conventional color gradient.

4.2. *Discussion*

Color gradients in early-type galaxies are believed to be due to metallicity and age gradients in the stellar population. The presence of dust produces increased reddening, while star for-

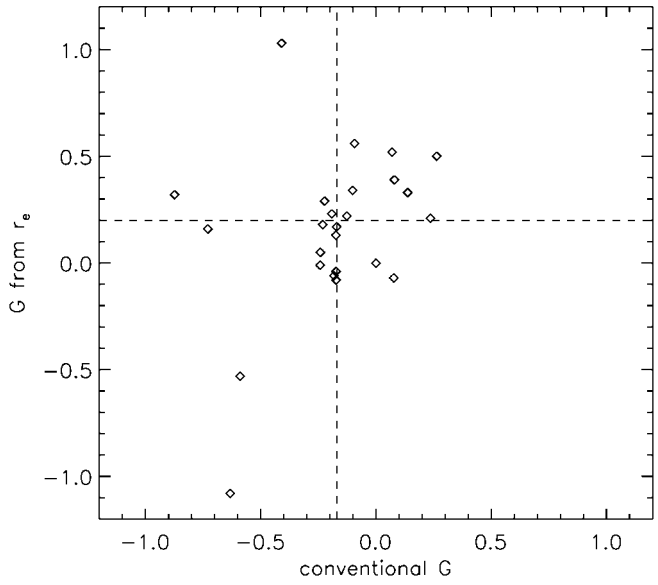

FIG. 3.—The conventional color gradient against the color variation as given by the *B* and *R* scale lengths for the radio galaxies. The latter is indicative of bluer central regions in many cases. A 2 × 2 contingency test shows that the two color indicators vary in the same sense.

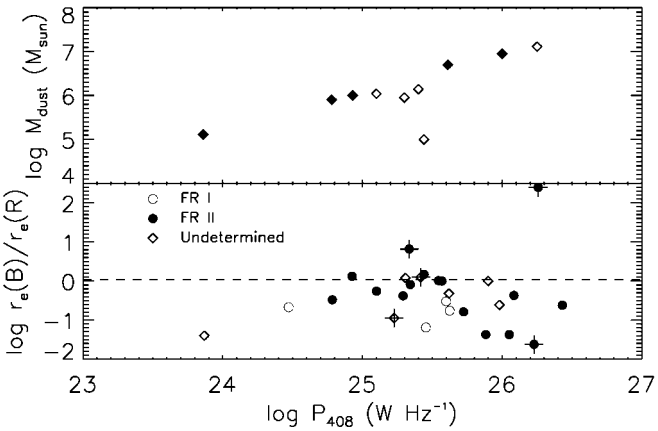

FIG. 4.—*Top*: correlation of dust mass in radio galaxies with dust lanes (*filled diamonds*) or dust patches (*open diamonds*) at the center with radio power. *Bottom*: $r_e(B)/r_e(R)$ as a function of radio power. The dashed line shows the scale length ratio expected for a normal galaxy. There is a hint that more powerful galaxies are bluer toward the center.

mation leads to bluer colors. In addition to any overall color gradient that we observe in the radio galaxies, their $B - R$ color images show regions of excess reddening indicative of dust. The dust occurs in the form of coherent lanes in ~20% of the galaxies, while another ~17% show dust patches. The remaining objects could of course contain dust well mixed with stars, which is not evident in the color maps. In several of the galaxies with $r_e(B)/r_e(R) > 1$, we see clear evidence of dust in the color maps. In the control galaxies, detectable dust again occurs in ~37% of the sample, but here the dust is more often patchy (30%).

Assuming that the composition of dust in the radio sample is similar to that in our Galaxy, and by using a simple screen model with a constant gas-to-dust ratio (see, e.g., Burstein & Heiles 1978), the mass of the dust can be estimated in the usual manner from the excess $B - R$ color. The dust mass turns out to be in the range of $\sim 10^5$–$10^7\ M_\odot$. A plot of dust mass against radio power (see Fig. 4) shows that the two are correlated, the linear correlation coefficient being significant at better than the 99% confidence level. The dust mass as well as the luminosity depend on the square of the distance, which could lead to a false correlation. The distance effect is probably not serious in the present case since the partial correlation coefficient, obtained after factoring out the distance, remains significant at better than the 90% level.

We have seen above that the distribution of the $r_e(B)/r_e(R)$ in the radio galaxies indicates that these objects more often become bluer toward the center than the control galaxies do. The blue color is presumably due to star formation, which is in some manner induced by the presence of the radio source. We have shown in Figure 4 a plot of the logarithm of the total radio power at 408 MHz against log $[r_e(B)/r_e(R)]$. It is seen that there is a clear trend for the more powerful radio galaxies to have steeper color gradients, as indicated by the scale length ratio. The more luminous a radio source is, the greater seems to be the increased blue luminosity triggered by it. Best, Longair, & Röttgering (1996) report finding either a string of bright star-forming knots or compact knots in the case of $z \sim 1$ radio galaxies from the 3CR catalog. These are thought to be produced by the interaction of the radio jet with the interstellar medium. It will be possible to model the mass and spatial extent of the gas involved in the bursts from narrowband imaging and long-slit spectra of the galaxies.

5. CONCLUSIONS

Using detailed model profile fits to the observed surface brightness profiles of samples of radio and control galaxies, we have shown that the distribution of the $r_e(B)/r_e(R)$ ratio is different for the two samples. A value less than 1 for this ratio in a galaxy indicates that the color of the galaxy becomes bluer toward the center, while $r_e(B)/r_e(R) > 1$ indicates that the color becomes redder toward the center. The ratio has a simple relation with the color gradient *G* obtained directly from color profiles. But the ratio can be used as an indicator of the radial dependence of color, even when the measured gradient is too noisy to serve the purpose.

REFERENCES

Best, P. N., Longair, M. S., & Röttgering, H. J. A. 1996, MNRAS, 280, L9
Burkert, A. 1993, A&A, 278, 23
Burstein, D., & Heiles, C. 1978, ApJ, 225, 40
Franx, M., Illingworth, G., & Heckman, T. 1989, AJ, 98, 538
Jedrzejewski, R. I. 1987, MNRAS, 226, 747
Mahabal, A. A. 1998, Ph.D. thesis, Pune Univ.
Mahabal, A. A., Kembhavi, A. K., & McCarthy, P. J. 1999, ApJ, submitted
Peletier, R. F., Davies, R. L., Davis, L. E., Illingworth, G. D., & Cawson, M. 1990, AJ, 100, 1091
Sandage, A., & Vishwanathan, N. 1978, ApJ, 223, 707
Smith, E. P., & Heckman, T. M. 1989, ApJ, 341, 658
Zirbel, E. 1996, ApJ, 473, 713